Chinese Journal of
POLYMER SCIENCE

RESEARCH ARTICLE

https://doi.org/10.1007/s10118-026-3740-4
Chinese J. Polym. Sci.

Exchange Kinetics of Reprocessable Vulcanization Networks Regulated by Inverse Vulcanization Copolymers

Zhou-Liang Wu[a], Ling-Rui Li[a], Yu Zhou[a], Di Yang[a], Shuang-Quan Liao[a], Jun-Fei Mei[b], Ai-Wu Ding[b*], and Ming-Chao Luo[a*]

[a] *School of Materials Science and Engineering, Hainan University, Haikou 570228, China*
[b] *Hainan Advanced Natural Rubber Composite Materials Engineering Research Center Co., Ltd., Chengmai 571924, China*

Abstract The reprocessing and recycling of vulcanized rubbers remain challenging because conventional vulcanization networks are irreversible. Here, we designed a modified sulfur crosslinker *via* inverse vulcanization to regulate the exchange kinetics of vulcanization networks, thereby governing the mechanical recovery behavior of reprocessed rubbers. Copolymers of sulfur and thioctic acid (CSTA), synthesized *via* inverse vulcanization, were employed to crosslink butadiene-styrene rubber. After vulcanization, thioctic acid (TA) introduces dynamic disulfide bonds into the conventional vulcanization networks, enabling thermally activated network rearrangement while preserving the overall crosslinked structure. Kinetic analysis revealed that increasing the TA content accelerated network exchange and significantly lowered the apparent activation energy for network rearrangements. Correspondingly, the recovery of the mechanical properties after reprocessing improved with increasing TA content. These results establish a clear correlation between vulcanization network exchange kinetics and macroscopic mechanical performance, providing a kinetic basis for the design of reprocessable vulcanization networks and offering a promising route toward recyclable high-performance rubber materials.

Keywords Reprocessable vulcanization networks; Inverse vulcanization copolymers; Network exchange kinetics

Citation: Wu, Z. L.; Li, L. R.; Zhou, Y.; Yang, D.; Liao, S. Q.; Mei, J. F.; Ding, A. W.; Luo, M. C. Exchange kinetics of reprocessable vulcanization networks regulated by inverse vulcanization copolymers. *Chinese J. Polym. Sci.* https://doi.org/10.1007/s10118-026-3740-4

INTRODUCTION

Rubbers are indispensable industrial resources that are widely used in tires, seals, vibration dampers, and many other engineering fields. Vulcanization is a necessary technology to impart rubber with practical properties.[1] However, covalent networks generated by vulcanization render vulcanized rubbers insoluble and infusible, making conventional vulcanized rubber extremely difficult to reprocess or recycle. In addition, the treatment of waste rubber often leads to serious environmental and resource concerns, such as landfilling[2] and energy-intensive pyrolysis.[3] Therefore, addressing the reprocessing and recycling of vulcanized rubbers while maintaining their mechanical integrity is an important prerequisite for the sustainable development of rubber materials.

In recent years, rapid progress in dynamic covalent chemistry has opened up new possibilities for reprocessable crosslinked rubbers. Dynamic bonds, such as reversible covalent bonds, ionic bonds, and hydrogen bonds, have been incorporated into elastomer networks to endow them with self-healing, reshaping, and recyclability.[4–8] For example, the Das' group[9] and Chen's group[10,11] have converted commercial rubbers into self-healing materials *via* ionic modification. Dynamic disulfide bonds,[12] β-hydroxyl esters,[13] and boronic esters[14] have also been successfully used to construct dynamic networks in commercial rubber. Although these studies convincingly demonstrate that dynamic cross-linking can make cross-linked rubbers self-healable and reprocessable, the prevailing strategy is to replace traditional vulcanization networks with designed dynamic networks. Given that vulcanization remains the dominant curing technology in the rubber industry, such approaches that rely on dynamic chemistry are difficult to implement in the practical rubber industry. Therefore, endowing traditional vulcanization networks with intrinsic reprocessability remains a key challenge in the rubber field.

Inverse vulcanization chemistry offers a promising new avenue for modifying conventional vulcanization networks. In recent years, Pyun and co-workers have developed a family of copolymerization reactions between elemental sulfur and organic comonomers, such as styrenic and (meth)acrylate monomers,[15,16] while Hasell *et al*. further expanded this reaction *via* tailored catalytic systems that lower the activation temperature and broaden the accessible monomer scope.[17,18] More recently, such inverse vulcanization copolymers have been demonstrated to act as efficient cross-linkers

* Corresponding authors, E-mail: dingaw@163.com (A.W.D.)
E-mail: mchluo@hainanu.edu.cn (M.C.L.)
Received April 3, 2026; Accepted May 6, 2026; Published online August 22, 2026

or modifiers for various rubbers, including diene rubbers,[19] Eucommia ulmoides gum,[20] and silica-filled elastomer composites.[21,22] These advances in inverse vulcanization chemistry and sulfur-rich copolymer design provide a conceptual and synthetic foundation for the present work on modifying traditional vulcanization networks.

In this study, we copolymerized sulfur and thioctic acid (TA) and employed the resulting inverse vulcanization TA copolymers (CSTA) to endow cross-linked rubbers with reprocessability. Specifically, CSTA prepared by inverse vulcanization was employed to crosslink butadiene-styrene rubber (SBR). This design enables commercial rubbers to maintain mechanical robustness while exhibiting reprocessability at elevated temperatures. With the increase in TA content in the vulcanization networks, the recovery rate of the mechanical performance improved. Moreover, increasing TA significantly reduces the apparent activation energy of network rearrangements. These findings reveal the key role of exchange kinetics in governing the mechanical recovery of reprocessed rubbers and provide a promising strategy for the design of reprocessable vulcanization networks in the rubber industry.

EXPERIMENTAL

Materials

Styrene-butadiene rubber (SBR) was purchased from Sinopec. Thiocic acid (99%, TA), *N*-methylimidazole (99%, NMI), 2,2′-dibenzothiazole disulfide (98%, DM), and stearic acid (SA) were purchased from Adamas. The accelerator, *N*-cyclohexyl-2-benzothiazolesulfenamide (98%, CZ), was purchased from Aladdin. Zinc oxide (ZnO) was also purchased from Macklin. Sulfur was obtained from Guangxi Fangchenggang Wuxing Environmental Technology Co., Ltd. All the reagents were used as received without further purification.

Synthesis of CSTA

Sulfur was added to a three-necked flask and heated to 150 °C until it was fully melted. Thioctic acid (TA) and NMI were added, and the mixture was stirred for 8 h. The reaction product was dissolved in THF (tetrahydrofuran), filtered, and concentrated by rotary evaporation. The mixture was then poured into water for extraction, and the precipitate was collected and dried to yield the inverse-vulcanized CSTA copolymer. CSTA samples with different compositions were synthesized by varying the feed ratio of sulfur to TA (7:3, 1:1, and 3:7).

Preparation of SBR Crosslinked by CSTA

SBR (100 g) was compounded on an open two-roll mill with SA (1 g), ZnO (5 g), CZ (1.5 g), and DM (0.5 g), and varying amounts of CSTA (1–6 g) were added sequentially. The total mixing time was about 15 min. The resulting compounds were then compression-molded at 160 °C under 15 MPa using the optimum curing time determined by a vulcameter in a mold with dimensions of 15 cm × 15 cm × 1 mm.

Characterizations

The chemical structure of CSTA was characterized using ^{1}H-NMR spectroscopy (Bruker Avance NEO 400) and Fourier transform infrared (FTIR) spectroscopy. For ^{1}H-NMR analysis, the samples were dissolved in dimethyl sulfoxide (DMSO) at room temperature. FTIR spectra were collected using an ATR-FTIR spectrometer (Bruker, Germany) in the range of 400–4000 cm^{-1}. The elemental compositions (C, H, N, O, and S) were determined using an Elementar Vario EL cube elemental analyzer. The glass transition temperature of SBR-CSTA was measured under a nitrogen atmosphere using a TA Instruments Q250 differential scanning calorimeter (DSC), following ISO 11357-2. The nitrogen flow rate was 50 mL/min and the heating rate was 10 °C/min over a temperature range from −80 °C to −20 °C. Tensile tests were conducted on a GOTECH AI-3000 universal testing machine to obtain stress-strain curves at a crosshead speed of 500 mm/min, following ISO 37. For tensile tests, 5 specimens were tested for each sample. The tested samples were first cut into small pieces and then reprocessed by compression molding at 160 °C and 15 MPa for 20 min. The same mold used in the initial molding process was employed for reprocessing, and the reprocessed samples were subjected to tensile testing using the same test method. The fracture energy (G_c) was measured at the rate of 6 mm/min. Before testing, a 1 mm notch was pre-cut at the center of the specimen. G_c was calculated using the following Eq. (1):

$$G_c = \frac{6Wc}{\sqrt{\lambda_c + 1}} \tag{1}$$

where λ_c (mm/mm) is the fracture strain of the notched specimen, c (mm) is the notch length, and W (J/m^3) is the integral area under the stress-strain curve of the unnotched specimen from strain 0 to λ_c.

Crosslinking density was determined using the equilibrium swelling method.[23–25] Samples were swollen in toluene at 25 °C for 7 days. The surface solvent was quickly removed with filter paper, and the swollen samples were weighed immediately. The samples were then dried to a constant weight in a vacuum oven at 80 °C to constant weight. The crosslinking density was calculated using Eqs. (2) and (3), respectively:

$$-\ln(1-\varphi_r) - \varphi_r - \chi_r\varphi_r^2 = nV_0\left(\varphi_r^{\frac{1}{3}} - \frac{1}{2}\varphi_r\right) \tag{2}$$

$$M_c = \frac{\rho}{n} \tag{3}$$

where φ_r is the volume fraction of polymer in the swollen network, V_0 is the molar volume of the solvent (toluene: 106.5 cm^3/mol), χ_r is the Flory-Huggins interaction parameter (0.393), n is the number of mobile chain segments per unit volume (mol/mL), M_c is the average molecular weight between crosslinks, and ρ is the density of the rubber.

Stress relaxation experiments were performed using a TA 850 dynamic mechanical analyzer (DMA) at 140, 150, 160, and 170 °C. Prior to testing, the samples were equilibrated at each temperature for 10 min to eliminate the influence of thermal expansion. A preload of 0.1 N was applied, followed by a 1% strain, and the stress evolution was recorded as a function of time. The characteristic relaxation time (τ) is defined as the time required for the stress to decay to 37% (1/e) of its initial value. The apparent activation energy for network rearrangements was calculated according to the Arrhenius equation.[26–28]

RESULTS AND DISCUSSION

Synthesis of CSTA

To endow conventional vulcanization networks with reprocess-

ability, we used the copolymerization of sulfur and TA to modify the sulfur. Copolymerization of sulfur and TA was carried out upon heating through inverse vulcanization (Fig. 1a, as evidenced by ^{1}H-NMR, FTIR, and DSC experiments. In Fig. 1(b), the signals around 3.5 ppm are assigned to the protons on the tertiary and secondary carbons adjacent to the S—S bond in the five-membered ring. The signals at round 1–2 ppm are attributed to the —CH_2 protons in the ring, whereas the signals around 2.2 ppm are assigned to the —CH_2 protons adjacent to the carboxyl group.[29,30] In the FTIR spectra (Fig. 1c), the carboxyl group of TA exhibits characteristic absorptions at approximately 3400 and 1700 cm^{-1}. Stretching vibrations of C—S (630 cm^{-1}) and S—S (490 cm^{-1}) in the polysulfide chains can be observed. Moreover, the DSC curve shows a glass transition at −30 °C (Fig. 1d), confirming the formation of CSTA. Furthermore, we regulated the composition of the CSTA by varying the feed ratio of sulfur to TA (7:3, 1:1, and 3:7). The TA content in CSTA, measured by an elemental analyzer, is 50%, 61.5%, and 72%, respectively, as shown in Fig. 1(e). SBR was compounded on an open two-roll mill with vulcanizing agents and varying amounts of CSTA.The synthesized CSTA are used to crosslink SBR, which is illustrated in Fig. 1(f).

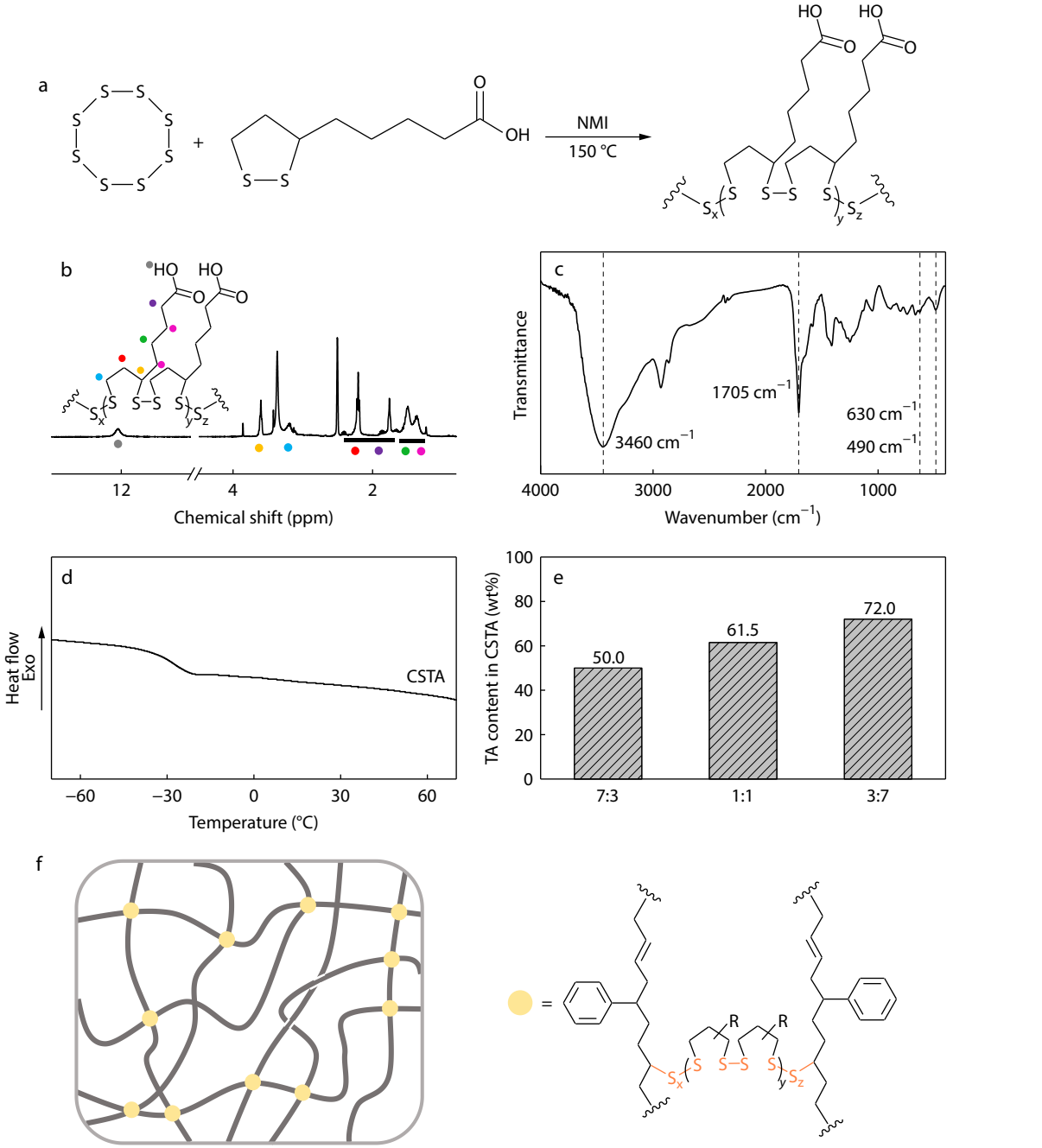

Fig. 1 The synthesis of CSTA. (a) The synthesis pathway of CSTA; (b) ^{1}H-NMR spectrum of CSTA; (c) FTIR spectrum of CSTA; (d) DSC curve of CSTA; (e) TA content in CSTA; (f) Schematic illustration of CSTA crosslinking SBR.

https://doi.org/10.1007/s10118-026-3740-4

Performance Analysis of SBR Crosslinked by CSTA

As shown in Fig. 2, CSTA with different TA contents were used to crosslink the SBR. The resulting vulcanizates are denoted as SBR-CSTA$_x$-y, where x is the ratio of TA to CSTA, and y is the weight fraction of CSTA per 100 g of SBR. Under the specific ratio of TA to CSTA, increasing the CSTA content significantly increased the torque in the torque-time curves in Figs. 2(a)–2(c). The crosslinking behaviors induced by CSTA were similar to those

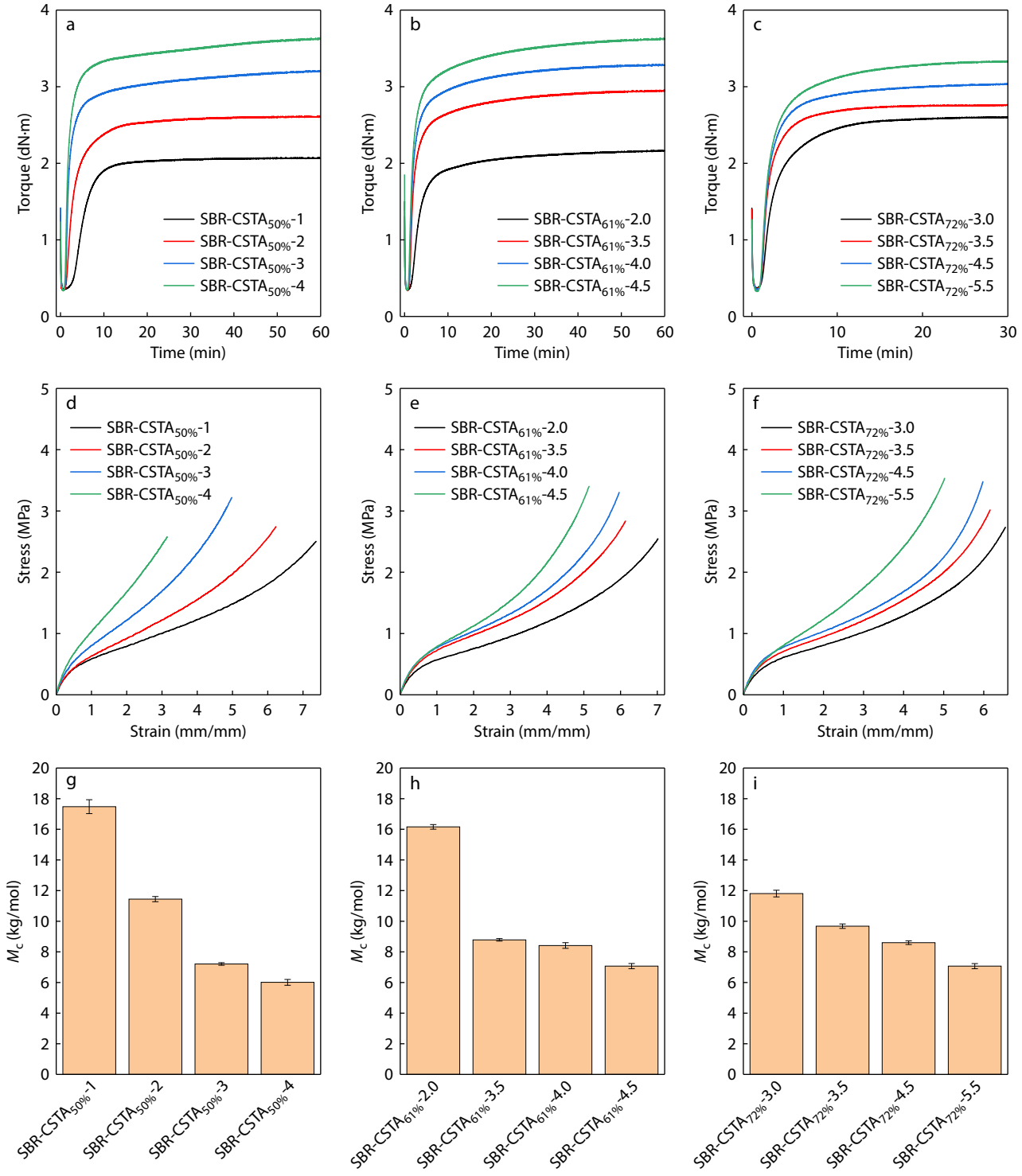

Fig. 2 Vulcanization and mechanical properties of SBR-CSTA. (a) Torque-time curves of SBR-CSTA$_{50\%}$ samples at 145 °C; (b) Torque-time curves of SBR-CSTA$_{61\%}$ samples at 145 °C; (c) Torque-time curves of SBR-CSTA$_{72\%}$ samples at 145 °C; (d) Stress-strain curves of SBR-CSTA$_{50\%}$ samples; (e) Stress-strain curves of SBR-CSTA$_{61\%}$ samples; (f) Stress-strain curves of SBR-CSTA$_{72\%}$ samples; (g) M_c of SBR-CSTA$_{50\%}$ samples; (h) M_c of SBR-CSTA$_{61\%}$ samples; (i) M_c of SBR-CSTA$_{72\%}$ samples.

https://doi.org/10.1007/s10118-026-3740-4

induced by traditional sulfur crosslinking.[31–33] SBR-CSTA samples also exhibit stress-strain responses comparable to those of typical vulcanized networks.[19] With increasing CSTA content, the tensile strength increased, whereas the elongation at break decreased, as shown in Figs. 2(d)–2(f). The crosslinking density of the SBR-CSTA samples was further determined using the equilibrium swelling method (Figs. 2g–2i). where M_c represents the average molecular weight of the two crosslinks. As the CSTA content increased, M_c decreased, indicating an increase in the crosslinking density, which accounted for the increased tensile strength and reduced elongation at break. An increased crosslinking density enhances the modulus and tensile strength but reduces the extensibility of the polymer chains, thereby leading to a decrease in the elongation at break, which is consistent with the tensile results of the samples.

Vulcanization Network Exchange Kinetics and Their Effects on Reprocessability

To compare the reprocessability of the SBR-CSTA samples, all materials in this section were prepared with an approximately identical crosslinking density of 7000 g/mol. Owing to the comparable crosslinking density, the samples exhibited similar stress-strain behaviors (Fig. 3a) and glass transition temperatures (Fig. 3b), indicating that the subsequent differences in toughness and reprocessability mainly arise from the nature and exchangeability of the crosslinks rather than from variations in crosslinking density. With increasing TA content in CS-

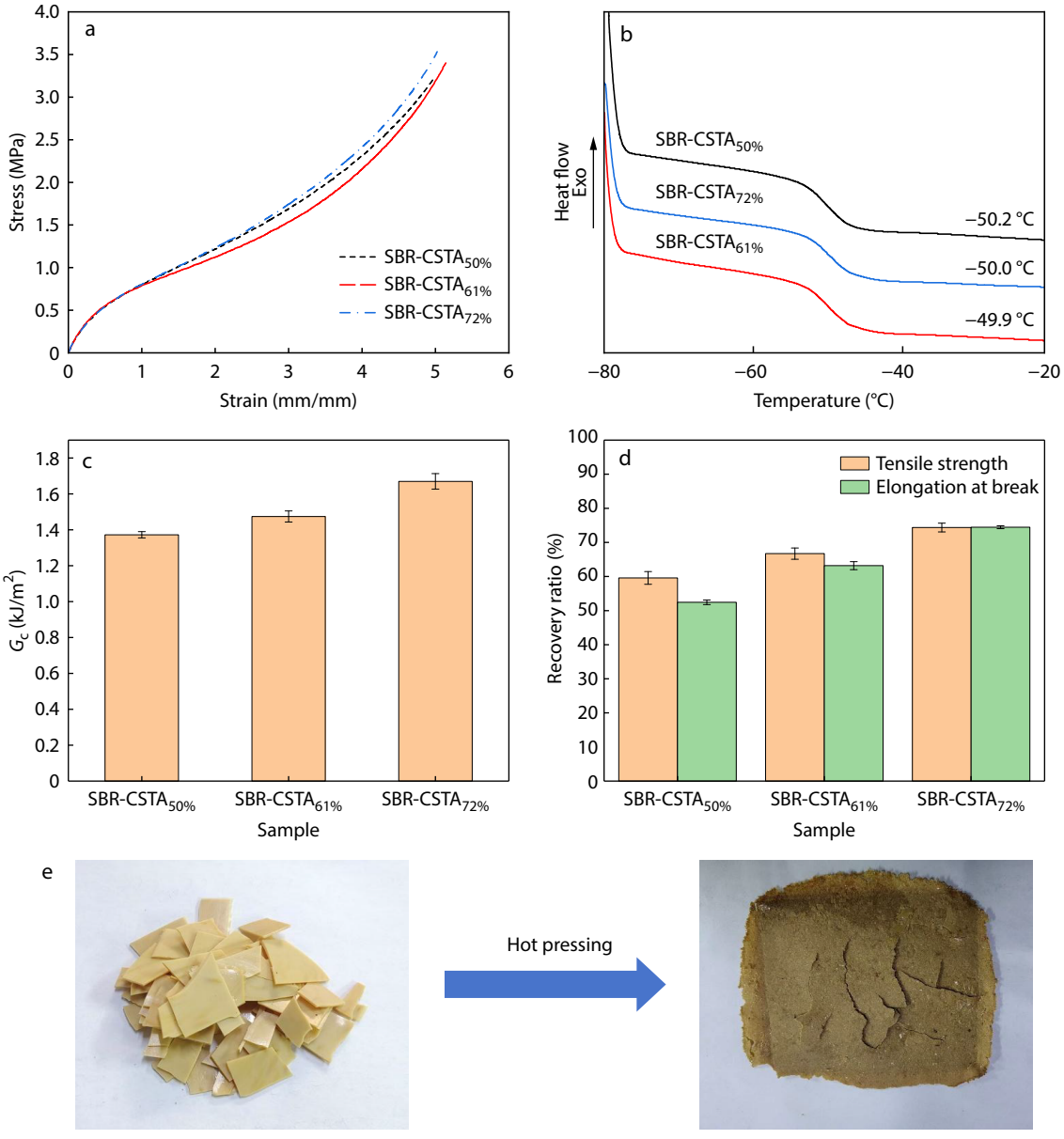

Fig. 3 Reprocessibility of SBR-CSTA samples with comparable crosslinking density; (a) Stress-strain curves of SBR-CSTA samples at a crosslinking density of about 7000 g/mol; (b) DSC curves of SBR-CSTA samples at a crosslinking density of about 7000 g/mol; (c) G_c of SBR-CSTA samples at a crosslinking density of about 7000 g/mol; (d) Changes in recovery of tensile strength and elongation at break for SBR-CSTA samples; (e) Images illustrate the changes of sulfur-cured SBR fragments treated by hot pressing.

https://doi.org/10.1007/s10118-026-3740-4

TA, the fraction of dynamic structural motifs in the network increases, and these dynamic bonds can undergo reversible exchange. This dynamic exchange enables stress redistribution and provides additional energy dissipation pathways, thereby further toughening the elastomers.[34–37] Accordingly, G_c in Fig. 3(c) increases with increasing TA content.

In addition to improving the toughness, the increased concentration of exchangeable motifs also promoted reprocessability. As shown in Fig. 3(d), the recovery rates of tensile strength and elongation at break after reprocessing both increase with increasing TA content, indicating that a higher density of dynamic exchangeable bonds facilitates more efficient network topology rearrangement during hot pressing. For comparison, a conventional sulfur-cured SBR was used as the control. The network of conventional sulfur-cured SBR is mainly composed of irreversible covalent crosslinks. Therefore, the network topology is essentially fixed and cannot undergo effective rearrangement during hot pressing, resulting in negligible reprocessability. After being cut into small pieces, the sulfur-cured SBR could not be consolidated into an intact specimen *via* hot-press molding, as shown in Fig. 3(e).

To investigate the kinetics of vulcanization network exchanges, we first used DMA to obtain the stress relaxation curves at different temperatures, as shown in Figs. 4(a)–4(c). All the samples with a crosslinking density of 7000 g/mol displayed characteristic stress relaxation curves, in which the stress gradually declined with increasing time. We then extracted the characteristic relaxation time (τ), defined as the time required for the relaxation modulus to decrease to 37% (1/e) of its initial value, and fitted the data using the Arrhenius equation in Fig. 4(d). From the Arrhenius plots, the apparent activation energies (E_a) for network exchange are determined to be 111.2, 95.7, and 87.7 kJ/mol for SBR-CSTA$_{50\%}$, SBR-CSTA$_{61\%}$, and SBR-CSTA$_{72\%}$, respectively (Fig. 4e). These results show that increasing the TA content significantly lowered the activation barrier for network rearrangement and accelerated dynamic bond exchange. It should be emphasized that E_a obtained from the Arrhenius analysis of stress relaxation represents an apparent activation energy for macroscopic network rearrangement, rather than the intrinsic activation energy of an isolated disulfide exchange reaction. Therefore, even though all SBR-CSTA samples contain TA-derived disulfide motifs, their E_a can differ because the concentration, distribution, accessibility, and local environment of these exchangeable motifs vary with the TA content. In a low-TA network, exchangeable sulfur bonds are relatively sparse and isolated; therefore, stress relaxation requires more cooperative rearrangement of larger network segments and less frequent effective exchange events. This results in slower re-

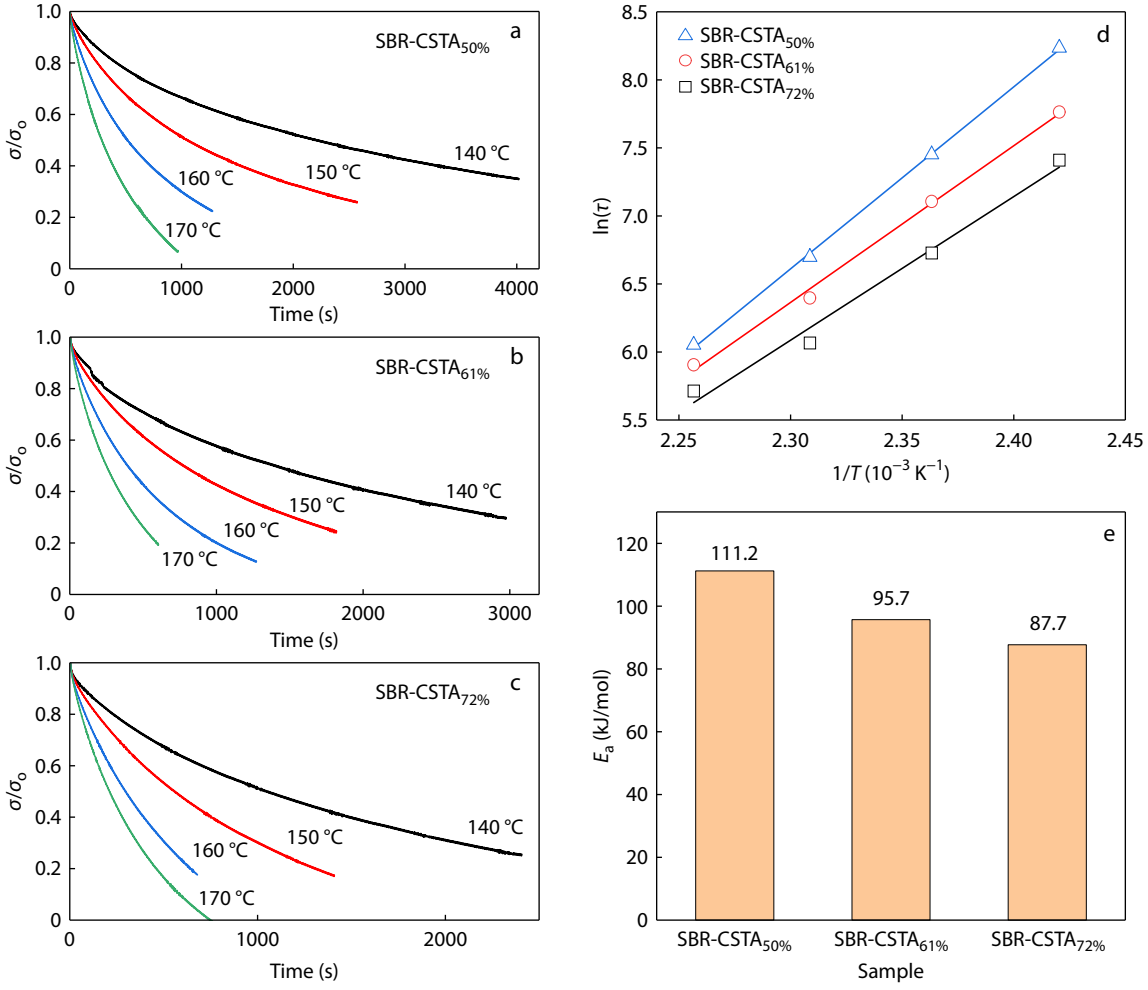

https://doi.org/10.1007/s10118-026-3740-4

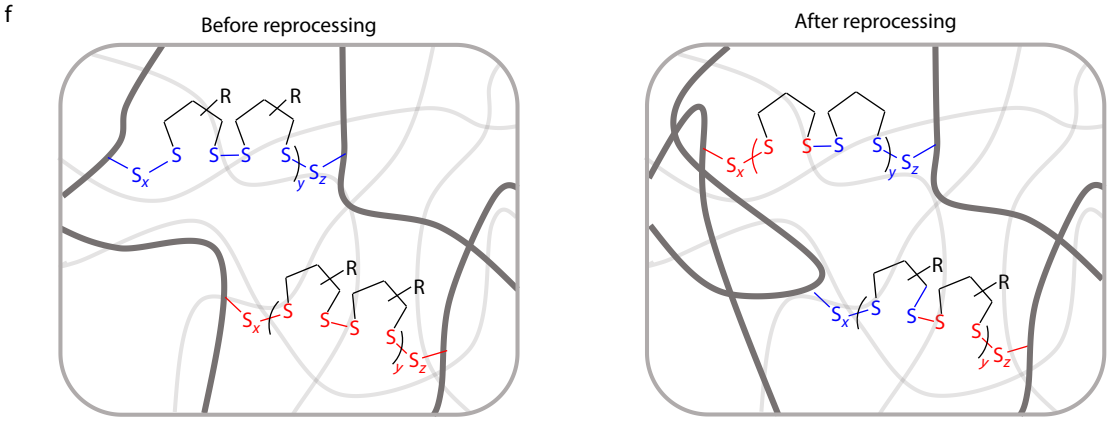

Fig. 4 Kinetic investigations of vulcanization network exchanges. (a) Stress relaxation curves of SBR-CSTA$_{50\%}$ at different temperatures; (b) Stress relaxation curves of SBR-CSTA$_{61\%}$ at different temperatures; (c) Stress relaxation curves of SBR-CSTA$_{72\%}$ at different temperatures; (d) Temperature dependence plots of relaxation time of SBR-CSTA$_{50\%}$, SBR-CSTA$_{61\%}$, and CSTA$_{72\%}$; Solid line represents the Arrhenius fitting curve and E_a is obtained by Arrhenius fitting; (e) E_a comparison among SBR-CSTA samples; (f) Image illustration of vulcanization network exchanges.

laxation and higher E_a. With increasing TA content, more dynamic disulfides were incorporated into the vulcanization network, providing a higher density of kinetically accessible exchange sites. Therefore, the network can rearrange through more local and frequent exchange events, leading to a faster stress relaxation and lower E_a. Accordingly, the decrease in E_a with increasing TA content reflects not only the presence of disulfide bonds but also the improved kinetic accessibility and higher concentration of exchangeable motifs in the CSTA-crosslinked networks. The lower apparent E_a and faster network exchange provide the kinetic basis for the improved reprocessability because a more rapidly rearranging network can more effectively reconstruct its topology during hot pressing. Fig. 4(f) schematically illustrates the exchange processes within the vulcanization network. Specifically, CSTA incorporates dynamic disulfide bonds into its network, imparting reprocessability. The presence of these disulfide bonds reduced the E_a required for network exchange, which is consistent with previous reports.[38,39]

CONCLUSIONS

In summary, modified sulfur was used to construct reprocessable vulcanization networks in rubbers. Through inverse vulcanization, the copolymerization of sulfur and TA introduces dynamic disulfide bonds into the sulfur. The resulting CSTA is used to crosslink SBR, enabling the formation of vulcanization networks with thermally activated exchangeability, thus imparting reprocessability to the vulcanized rubber. With an increase in the TA content, the recovery rate of the mechanical performance improved. Moreover, a higher TA content reduces the apparent activation energy, facilitating dynamic bond exchange. This study presents an effective strategy for designing reprocessable vulcanization networks and offers new insights into the development of sustainable rubber materials.

Conflict of Interests

The authors declare no interest conflict.

Data Availability Statement

The data that support the findings of this study are available from the corresponding author upon reasonable request. The contact information of corresponding author: mchluo@hainanu.edu.cn.

ACKNOWLEDGMENTS

This study was financially supported financially by the National Natural Science Foundation of China (No. 52363007).

REFERENCES

1 Akiba, M.; Hashim, A. S. Vulcanization and crosslinking in elastomers. *Prog. Polym. Sci.* **1997**, *22*, 475–521.
2 Chittella, H.; Yoon, L. W.; Ramarad, S.; Lai, Z. W. Rubber waste management: A review on methods, mechanism, and prospects. *Polym. Degrad. Stabil.* **2021**, *194*, 109761–109782.
3 Bowles, A. J.; Fowler, G. D.; O'Sullivan, C.; Parker, K. Sustainable rubber recycling from waste tyres by waterjet: A novel mechanistic and practical analysis. *Sustainable Mater. Technol.* **2020**, *25*, e00173.
4 Webber, M. J.; Tibbitt, M. W. Dynamic and reconfigurable materials from reversible network interactions. *Nat. Rev. Mater.* **2022**, *7*, 541–556.
5 Lei, Z.; Chen, H.; Huang, S.; Wayment, L. J.; Xu, Q.; Zhang, W. New advances in covalent network polymers *via* dynamic covalent chemistry. *Chem. Rev.* **2024**, *124*, 7829–7906.
6 Maes, S.; Badi, N.; Winne, J. M.; Du Prez, F. E. Taking dynamic covalent chemistry out of the lab and into reprocessable industrial thermosets. *Nat. Rev. Chem* **2025**, *9*, 144–158.
7 Zu, Z. J.; Cao, Y. Y.; Liu, J. W.; Lin, Z. Q.; Zhang, L. Y.; Xiang, H. P.; Zhang, M. Q. Self-healing, reprocessable, and antibacterial silicone rubber enabled by ionic crosslinking bonds. *Acta Polymerica Sinica* (in Chinese) **2025**, *56*, 152–165.
8 Ye, J.; Zu, Z. J.; Lin, Z. Q.; Xiang, H. P.; Zhang, M. Q. Intrinsic self-healing polysiloxane materials: From single dynamic crosslinked network to multiple dynamic crosslinked networks. *Acta Polymerica Sinica* (in Chinese) **2023**, *54*, 1028–1054.
9 Das, A.; Sallat, A.; Böhme, F.; Suckow, M.; Basu, D.; Wießner, S.; Stöckelhuber, K. W.; Voit, B.; Heinrich, G. Ionic modification turns commercial rubber into a self-healing material. *ACS Appl. Mater.*

Graphical Abstract

Exchange Kinetics of Reprocessable Vulcanization Networks Regulated by Inverse Vulcanization Copolymers

Zhou-Liang Wu, Ling-Rui Li, Yu Zhou, Di Yang, Shuang-Quan Liao, Jun-Fei Mei, Ai-Wu Ding, and Ming-Chao Luo

Hainan University; Hainan Advanced Natural Rubber Composite Materials Engineering Research Center Co., Ltd.

Copolymers of sulfur and thioctic acid are employed to regulate exchange kinetics in vulcanization networks. Increasing the thioctic acid content lowers the apparent activation energy for network rearrangement.

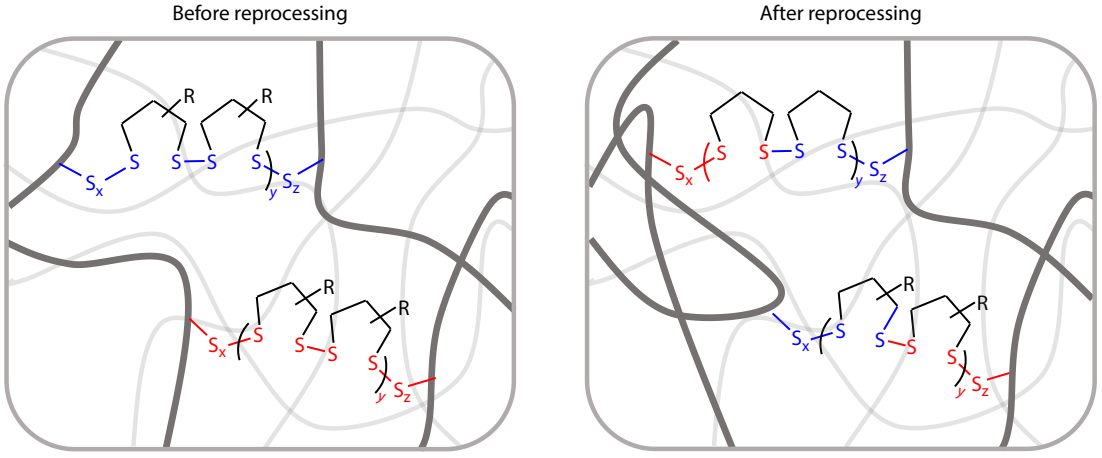

Chinese J. Polym. Sci. 2026 *https://doi.org/10.1007/s10118-026-3740-4*

Interfaces **2015**, *7*, 20623−20630.

10 Xu, C.; Cao, L.; Huang, X.; Chen, Y.; Lin, B.; Fu, L. Self-healing natural rubber with tailorable mechanical properties based on ionic supramolecular hybrid network. *ACS Appl. Mater. Interfaces* **2017**, *9*, 29363−29373.

11 Xu, C.; Cao, L.; Lin, B.; Liang, X.; Chen, Y. Design of self-healing supramolecular rubbers by introducing ionic cross-links into natural rubber *via* a controlled vulcanization. *ACS Appl. Mater. Interfaces* **2016**, *8*, 17728−17737.

12 Cheng, B.; Lu, X.; Zhou, J.; Qin, R.; Yang, Y. Dual cross-linked self-healing and recyclable epoxidized natural rubber based on multiple reversible effects. *ACS Sustainable Chem. Eng.* **2019**, *7*, 4443−4455.

13 Tang, Z.; Liu, Y.; Guo, B.; Zhang, L. Malleable, mechanically strong, and adaptive elastomers enabled by interfacial exchangeable bonds. *Macromolecules* **2017**, *50*, 7584−7592.

14 Chen, Y.; Tang, Z.; Liu, Y.; Wu, S.; Guo, B. Mechanically robust, self-healable, and reprocessable elastomers enabled by dynamic dual cross-links. *Macromolecules* **2019**, *52*, 3805−3812.

15 Lee, T.; Dirlam, P. T.; Njardarson, J. T.; Glass, R. S.; Pyun, J. Polymerizations with elemental sulfur: From petroleum refining to polymeric materials. *J. Am. Chem. Soc.* **2022**, *144*, 5−22.

16 Bao, J.; Martin, K. P.; Cho, E.; Kang, K. S.; Glass, R. S.; Coropceanu, V.; Bredas, J. L.; Parker, W. O., Jr.; Njardarson, J. T.; Pyun, J. On the mechanism of the inverse vulcanization of elemental sulfur: Structural characterization of poly(sulfur-random-(1,3-diisopropenylbenzene)). *J. Am. Chem. Soc.* **2023**, *145*, 12386−12397.

17 Dodd, L. J.; Omar, Ö.; Wu, X.; Hasell, T. Investigating the role and scope of catalysts in inverse vulcanization. *ACS Catal.* **2021**, *11*, 4441−4455.

18 Wu, X.; Smith, J. A.; Petcher, S.; Zhang, B.; Parker, D. J.; Griffin, J. M.; Hasell, T. Catalytic inverse vulcanization. *Nat. Commun.* **2019**, *10*, 647.

19 Wang, D.; Tang, Z.; Liu, Y.; Guo, B. Crosslinking diene rubbers by using an inverse vulcanised co-polymer. *Green Chem.* **2020**, *22*, 7337−7342.

20 Ni, Q.; Wu, J.; Kong, P.; Wang, Y.; Li, Y.; Li, Y.; Peng, X. Inverse vulcanization polymer-modified eucommia ulmoides gum with enhanced shape memory capability and sound absorption property. *ACS Appl. Polym. Mater.* **2022**, *4*, 4689−4698.

21 Wang, D.; Chen, J.; Tang, Z.; Huang, R.; Xiao, Y.; Chen, J.; Yin, P.; Guo, B.; Zhang, L. Exploring epoxy-functionalized polysulfide as a VOC-free and highly effective interfacial modifier for silica-filled rubber composites. *Macromolecules* **2024**, *57*, 470−480.

22 Wang, D.; Tang, Z.; Huang, R.; Li, H.; Zhang, C.; Guo, B. Inverse vulcanization of vinyltriethoxysilane: A novel interfacial coupling agent for silica-filled rubber composites. *Macromolecules* **2022**, *55*, 8485−8494.

23 Ellis, B.; Welding, G. N. Estimation, from swelling, of the structural contribution of chemical reactions to the vulcanization of natural rubber. Part II. estimation of equilibrium degree of swelling. *Rubber Chem. Technol.* **1964**, *37*, 571−575.

24 Vieyres, A.; Pérez-Aparicio, R.; Albouy, P.-A.; Sanseau, O.; Saalwächter, K.; Long, D. R.; Sotta, P. Sulfur-cured natural rubber elastomer networks: Correlating cross-link density, chain orientation, and mechanical response by combined techniques. *Macromolecules* **2013**, *46*, 889−899.

25 Wu, Z. L.; Guo, H. J.; Li, L. R.; Liao, S.; Luo, M.-C. A hybrid cross-linking point strategy to reconcile reprocessability and creep resistance in mechanically robust rubbers. *Macromolecules* **2026**, *59*, 1499−1507.

26 Isogai, T.; Hayashi, M. Critical effects of branch numbers at the cross-link point on the relaxation behaviors of transesterification vitrimers. *Macromolecules* **2022**, *55*, 6661−6670.

27 Guerre, M.; Taplan, C.; Nicolaÿ, R.; Winne, J. M.; Du Prez, F. E. Fluorinated vitrimer elastomers with a dual temperature response. *J. Am. Chem. Soc.* **2018**, *140*, 13272−13284.

28 He, C.; Christensen, P. R.; Seguin, T. J.; Dailing, E. A.; Wood, B. M.; Walde, R. K.; Persson, K. A.; Russell, T. P.; Helms, B. A. Conformational entropy as a means to control the behavior of poly(diketoenamine) vitrimers in and out of equilibrium. *Angew. Chem. Int. Ed.* **2020**, *59*, 735−739.

29 Shi, C. Y.; Zhang, Q.; Wang, B. S.; Chen, M.; Qu, D. H. Intrinsically photopolymerizable dynamic polymers derived from a natural small molecule. *ACS Appl. Mater. Interfaces* **2021**, *13*, 44860−44867.

30 Yu, S.; Tang, Z.; Wang, D.; Guo, B.; Zhang, L. Toughening rubber by *in situ* construction of hierarchical coordination complexes with a sulfur-based ionomer. *Macromolecules* **2024**, *57*, 10120−10129.

31 Wei, Y. C.; Liu, G. X.; Zhang, H. F.; Zhao, F.; Luo, M. C.; Liao, S. Non-rubber components tuning mechanical properties of natural rubber from vulcanization kinetics. *Polymer* **2019**, *183*, 121911.

32 Wei, Y. C.; Liu, G. X.; Zhang, L.; Zhao, F.; Liao, S.; Luo, M. C. Exploring the unique characteristics of natural rubber induced by coordination interaction between proteins and Zn^{2+}. *Polymer* **2020**, *193*, 122357.

33 Kong, L.; Zhang, J.; Huang, S.; Zhang, R.; Li, J.; Xie, Z.; Wu, J. Designing highly entangled, homogeneous, and low-defect networks for high-performance rubbers. *Macromolecules* **2025**, *58*, 3109−3118.

34 Xiao, Y.; Li, Q.; Yao, X.; Bai, R.; Hong, W.; Yang, C. Fatigue of amorphous hydrogels with dynamic covalent bonds. *Extreme Mech. Lett.* **2022**, *53*, 101679.

35 Chen, X.; Lin, J.; Yang, H.; Tang, J. Flaw sensitivity of hydrogels with dynamic covalent bonds. *Extreme Mech. Lett.* **2024**, *67*, 102129.

36 Yang, H.; Chen, X.; Sun, B.; Tang, J.; Vlassak, J. J. Fracture tolerance induced by dynamic bonds in hydrogels. *J. Mech. Phys. Solids* **2022**, *169*, 105083.

37 Hu, B. X.; Guo, H. J.; Pan, X.; Liao, S.; Luo, M. C. Tough, fatigue-resistant elastomer networks *via* dynamic interactions. *ACS Appl. Polym. Mater.* **2025**, *7*, 5173−5179.

38 Li, X.; Bai, J.; Yu, B.; Chen, F.; Tian, M. Combination of dynamic and permanent cross-linking: A pathway to enhance elasticity and recyclability. *ACS Appl. Mater. Interfaces* **2025**, *17*, 18971−18980.

39 Zhao, J.; Zhang, Z.; Wang, C.; Yan, X. Synergistic dual dynamic bonds in covalent adaptable networks. *CCS Chem.* **2024**, *6*, 41−56.

https://doi.org/10.1007/s10118-026-3740-4